

Article

The Use of Geomaterials to Restore the Utility Value of Post-Mining Areas

Dagmara Perzyło¹, Katarzyna Szafulera^{1,*} , Marek Kruczkowski¹ and Michał Pilch²

¹ Faculty of Mining, Safety Engineering and Industrial Automation, Silesian University of Technology, ul. Akademicka 2a, 44-100 Gliwice, Poland; dagmara.perzylo@polsl.pl (D.P.); marek.kruczkowski@polsl.pl (M.K.)

² The Realization Company INORA sp.z o.o., ul. Prymasa Wyszyńskiego 11, 44-100 Gliwice, Poland; michal.pilch@op.pl

* Correspondence: katarzyna.szafulera@polsl.pl

Abstract: Post-mining deformations that occur on the surface pose a significant threat to natural environments and urbanized areas. Preventing the effects of deformation is a significant challenge for specialists in geotechnical and civil engineering. Geomaterials, such as geosynthetics or geopolymers, could minimize the damage that occurs. The first section of the article explores the securing of an area, strengthening the rock mass with geosynthetic materials. We provide descriptions of the properties of these materials and the method surrounding their introduction into the soil. The second section presents the research problem, i.e., we describe the damage caused by underground mining. In the last section, we propose a solution for securing the ground with the use of geogrids and geopolymer injections into the rock mass. The analyses led us to conclude that an area subjected to mining influences may be strengthened by the use of geosynthetic materials. The use of geosynthetics in a mining area is a well-known topic, but the additional use of geopolymers may be innovative. Research is still being conducted on the use of geopolymers to fill post-mining voids, in combination with geosynthetics.

Keywords: underground extraction; post-mining subsidence; geosynthetic materials; geotechnics



Citation: Perzyło, D.; Szafulera, K.; Kruczkowski, M.; Pilch, M. The Use of Geomaterials to Restore the Utility Value of Post-Mining Areas. *Energies* **2022**, *15*, 1447. <https://doi.org/10.3390/en15041447>

Academic Editors: Rao Martand Singh and F. Pacheco Torgal

Received: 22 November 2021

Accepted: 13 February 2022

Published: 16 February 2022

Publisher's Note: MDPI stays neutral with regard to jurisdictional claims in published maps and institutional affiliations.



Copyright: © 2022 by the authors. Licensee MDPI, Basel, Switzerland. This article is an open access article distributed under the terms and conditions of the Creative Commons Attribution (CC BY) license (<https://creativecommons.org/licenses/by/4.0/>).

1. Introduction

In the Polish Upper Silesian Coal Basin, underground coal mining is often carried out in urbanized areas, resulting in damage to buildings, communication, and technical infrastructure. Geomechanical transformations of land surfaces mainly constitute continuous deformations in the form of subsidence troughs, which may be accompanied by discontinuous linear and surface deformations [1–8]. Based on previous studies regarding the occurrence of discontinuous deformations, a significant predominance was found in the occurrence of linear deformations over surface deformations [9,10]. Preventing their effects is a significant challenge for specialists in geotechnical and civil engineering.

In [11,12], the authors present several different solutions to this problem. Among the geomaterials, one can distinguish, inter alia, geotextiles, geogrids, geonets, etc. [13]. In this paper, we paid special attention to geogrids, which may be used for:

- Construction of reinforced embankments and retaining structures.
- Strengthening the upper subsoil layer of road surfaces.
- Strengthening the weak subsoil of road embankments and protective dikes.
- Reinforcement of the bottom layers of the foundation.

Geopolymers have completely different properties. These materials are primarily expansive resins that can be injected into the soil, to:

- Improve the load-bearing capacity of the subsoil and foundation and its reinforcement (filling, compaction, and consolidation).
- Provide structural support (filling voids).

As previously mentioned, there are various threats (from mining exploitations) in mining and post-mining areas [4–10]. Keep in mind that mining excavations are often carried out under urbanized areas with technical and communication infrastructures. To protect existing facilities and secure new structures, various security measures should be employed. Regarding road surfaces, protective measures in the form of geogrids may be employed, especially in cases where additional threats are expected, e.g., in the shape of discontinuous deformations related to tectonic faults and shallow mine workings [10]. Geogrids do not always give sufficient barriers, e.g., regarding the risks of discontinuous deformations arising. In such cases, geopolymers can be additionally used to strengthen a facility, to be protected.

In Poland, numerous experiences exist in the field of road protection, with the use of geogrids in mining areas. The first example involves the protection of the road embankment in Jastrzębie-Bzie, with the use of geomattresses [14]. This is an example of one of the best solutions in Poland. Moreover, there is an example of protection with the A4 motorway geomattress, which was not properly constructed and, as a result, damage to it occurred [15]. Another example concerns the lack of protection on the A4 motorway, which resulted in a “ground step” around the tectonic dislocation [16–18]. The road required renovation with the use of geogrids. A similar problem concerns national road number 44 [6]. Numerous linear (and discontinuous) deformations appeared on the road in the past, relating to mining operations in the vicinity of tectonic faults, despite the use of geogrids. This problem was related to the lack of additional treatments (e.g., injections) reducing the risk of tectonic dislocation activation, which usually resulted in damage to urban facilities. Protection with geogrids was also applied in cases when discontinuous linear deformations were created in the vicinity of the shaft [19].

The problem with securing the A1 motorway in the Piekary junction area was solved completely differently [20,21]. The risk of discontinuous deformations was eliminated here by filling the voids and relaxation zones, via the borehole injection method, to seal and strengthen the rock mass, and then geogrids were used. Among the works related to the use of geogrids in securing roads against the effects of mining exploitation, the following works should be mentioned: [22–29].

Based on the presented review of the bibliography, it was found that geogrids have been used in the existing safeguards in mining areas, while there is no experience with the use of geogrids and geopolymers simultaneously. These materials, having certain properties, such as high strength, low mass, lack of chemical reactions with the rock environment, can successfully act as factors preventing the formation and development of already existing discontinuous deformations.

Compared to the works related to the research topic—a similar solution was presented in previously mentioned works [17], while additionally, the possibility of using a geopolymer was considered. This could be justified by minimizing the risk of future linear deformations. The geogrid should protect the surface from horizontal tensile strain, while the geopolymer fills the fault gap. This paper—based on the analysis of mining conditions and surface transformations caused by underground mining—presents a proposal for the treatment of an area intended for development with the use of geopolymers and geogrids.

2. Area Protection and Improvement of Soil Bearing Capacity

To improve the quality of the area where underground mining is carried out, synthetic materials, such as geopolymers or geosynthetics (including geogrids), could be used. Geopolymers introduced into the rock mass will fill the voids formed by discontinuous linear deformations, while geogrids will additionally protect the area.

2.1. Geosynthetics

2.1.1. Origin of the Use of Geosynthetics

Reinforcement of soil with geosynthetics has been known about since ancient times. In the past, the soil was reinforced with reeds; today, it is done with geosynthetics. By

using geosynthetic reinforcement, a composite is created that is characterized by a specific tensile strength that the soil itself does not have. Geosynthetics are currently used in various types of construction objects, such as retaining walls, bridge abutments, or road embankments. Geosynthetics are also successfully used as horizontal reinforcements over columns or piles, or, as described in this paper, horizontal reinforcements over various types of anomalies in the subsoil layers in the form of sinkholes, voids, or tectonic faults, where injections of geopolymer materials may be applied. In such cases, in order to reinforce the subsoil under a construction object, it is necessary to combine two reinforcing procedures: filling in the cracks in the ground with a grout, e.g., a geopolymer, followed by the application of a horizontal reinforcement at the ground surface level. This type of technology has already been successfully used to reinforce the soil, e.g., under road or railway embankments. From the point of view of geosynthetic reinforcement, in this type of structure, the failure mechanism usually induces tension in the structure, which is counteracted by the installed geosynthetics.

2.1.2. Tensile Strength of Geosynthetics as a Basic Parameter

For geosynthetics used as horizontal reinforcements, numerically expressed tensile strength is an important parameter, from the point of view of static calculations. This parameter belongs to the group of principal parameters. A distinction is made between the characteristic short-term strength— $F_{o,k}$, the long-term design strength— F_d , and the characteristic long-term tensile strength— $F_{k,\epsilon}$. The short-term strength ($F_{o,k}$) is the strength of a 20 cm wide strip tested at 20%/min, according to PN-EN ISO 10,319 [30], this is a guaranteed value with a confidence level of 95%, and it can be read off the labels or the manufacturer's delivery documentation. F_d is the strength determined, taking into account all impacting forces at the point of rupture of the geosynthetic. This strength refers to the limit state I. $F_{k,\epsilon}$ is the characteristic tensile strength for the allowable total elongation of the reinforcement (ϵ_{gr}) from the time of integration to the end of life of the facility. This strength refers to limit state II.

2.1.3. Polymers Used in the Production of Geosynthetics

In the production process, the type of polymer used to manufacture the geosynthetic product is also important in terms of strength parameters. Geosynthetics are currently manufactured from a wide range of polymers, but the following are most commonly used for the purposes of soil reinforcement: aramid (AR), polyvinyl alcohol (PVA), polyester (PES, PET), polyamide (PA), polypropylene (PP), and high density polyethylene (PEHD). These polymers show sufficient resistance in natural soil and water environments with a pH in the range of $4 \div 9$. In the pH range >9 , only geosynthetics used with AR or PVA are used for reinforcement. Geosynthetics can be divided into the following most common groups: flat and spatial geogrids, geotextiles, and geocomposites, which are a combination of geogrids and geofabrics or geogrids and geotextiles, geocells.

2.1.4. Guidelines and Standards

Many years of practice, in the application of geosynthetic reinforcements, has allowed engineers and scientists to work out standards and guidelines for application of geosynthetic technologies, to improve the quality of soil, including areas affected by mining exploitation.

For geotechnical design and calculation of geosynthetic reinforcement, Eurocode 7 [31] and the so-called national annexes, e.g., (in Poland) Instruction ITB 429/2007 [32], may be used. For example, in Germany, new standards, DIN 1054:2010 [33] and DIN 4084:2009 [34], are applied, which complement the provisions of EC 7 [31] in the scope of geotechnical design. In 2010, EBGEO recommendations [35] were issued, so, with the introduction of EC 7 [31] and DIN 1054:2010 [33], a coherent standard system could be established in Germany, including designs with geosynthetics. In the UK, the BS standard was revised with a new version, BS 8006:2010 [36]. In France, two standards were issued for the

design of reinforced soil structures: NF P 94-270:07.2009 [35] and XP G 38-064:2010 [37], which are also based on the limit state method. Nevertheless, it is not advisable to mix recommendations issued in different countries, but to follow one accepted standard, from the beginning of the design until the end of the construction. In spite of similar algorithms and factors, mixing different design systems may lead to errors in the form of uneconomical oversizing of structures, or worse, their under-sizing.

2.1.5. Limit State Method: First Ultimate Limit State

In a view of the failure mechanism causing elongation of the structure, e.g., at the base of an embankment over the aforementioned anomalies in the soil, dimensioning must be carried out according to the limit state method. Thus, first of all, the design tensile strength of geosynthetics at the ultimate limit state I should be determined. In accordance with [32], the formula (1) is used:

$$F_d = \frac{F_{o,k}}{A_1 * A_2 * A_3 * A_4 * \gamma_F} \quad (1)$$

where:

F_d —long-term design strength, kN/m;

$A_1 \dots 4$ —material coefficients, taking into account the impact of the creep, mechanical damage, loss of strength at joints, impact of water, and ground environment;

$F_{o,k}$ —characteristic value of tensile strength, kN/m;

γ_F —material safety factor.

2.1.6. Second Ultimate Limit State

For the verification of the second limit state, Formula (2) is used:

$$|s| \leq |s|_{gr} \quad (2)$$

where:

$|s|$ —value of subsidence or subsidence differences, m;

$|s|_{gr}$ —limit value of deformation, m.

Verification of the serviceability limit state can be carried out by checking the strain of reinforcement, which is expressed by the Equation (3):

$$\varepsilon \leq \varepsilon_{gr} \quad (3)$$

where:

ε —maximum value of reinforcement strain, considering the creep during the design life of the structure, %;

ε_{gr} —allowable amount of strain, %.

In terms of the second serviceability limit state, for the purpose of checking the allowable elongation of geosynthetic reinforcement, the isochrones (isolines of the elongation of the geosynthetic material in time) were used (Figure 1). From the isochrons, it is possible to read the value of the strength utilization rate of the geosynthetic reinforcement β for a given time t , and the allowable elongation ε . In practice, the maximum reinforcement lifetime $t = 120$ years is specified, and the value of the allowable strain is read from standards or guidelines (e.g., Instruction ITB 429/2007 [32]).

2.1.7. Example of Application of Geosynthetics as Horizontal Reinforcement

One example involving the use of geosynthetics as horizontal reinforcements may be a sinkhole, e.g., in the form of a funnel of a specific diameter, or a fault of a specific height. In such cases, filling the resulting voids is usually considered. For example, geopolymer filling can be used. Horizontal geosynthetic reinforcement is used to transfer all loads and ensure the continuous exploitation of the area above the void or sinkhole in cases when the filling of the void alone proves to be insufficient. Such a situation can occur, for example, with further movements of the rock mass. Chapter 11 of the EBGeo [35] deals with such issues. In accordance with [35], the respective elongation limits of reinforcement elements (geosynthetics) are determined, the dimensioning of which should be carried out

within the framework of the ultimate limit state I and serviceability limit state II (as above). Elongations and forces mobilized in geosynthetic reinforcements can be monitored with an appropriate monitoring system, which makes it possible to control the operation of the structure. A properly designed monitoring system makes it possible to monitor whether we are approaching the established alarm states. This gives us additional time to take possible preventive and repair actions.

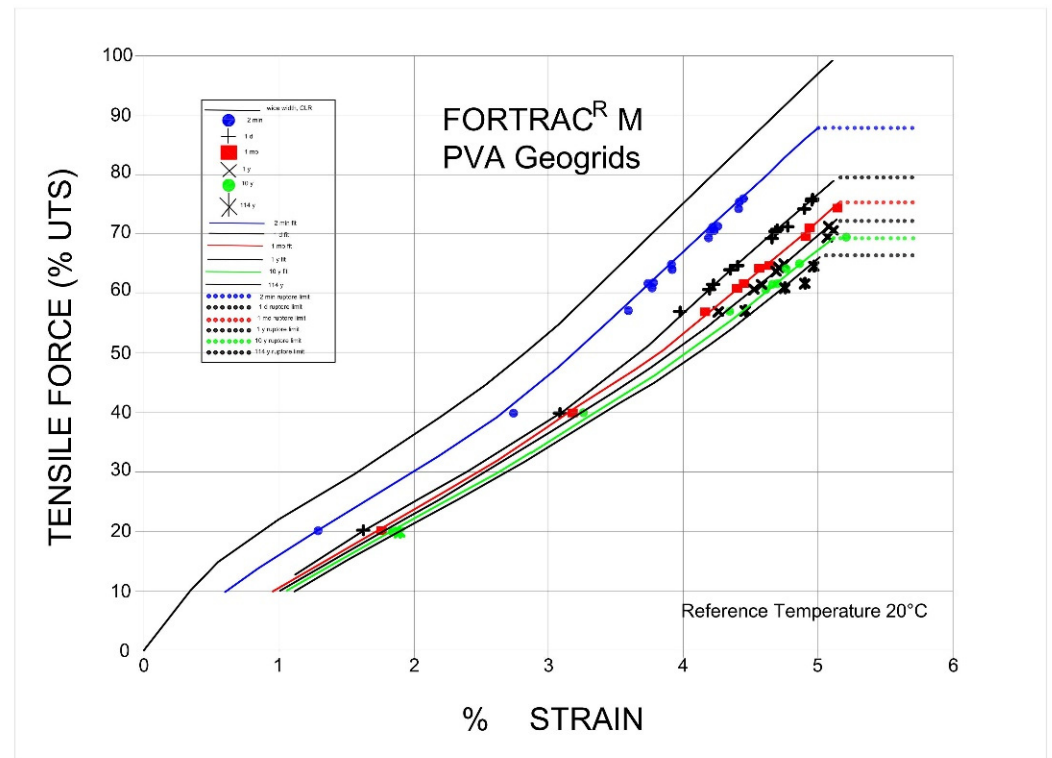


Figure 1. Example isochrones of PVA geogrids. Adapted from [38].

In approaching the above-mentioned issues, for example, the BS 8006:1995 standard can be used, along with Perrier's graphical method [39], and the RAFAEL method, developed on the basis of field simulations in France [40]. The main differences between the methods used involve the different descriptions of the behaviors of the soil over the resulting sinkhole or the impact of the form of the sinkhole on the work of the geosynthetic reinforcement. The RAFAEL method assumes that the sinkhole has a circular shape of a certain diameter D when viewed from above and is covered by a reinforcement installed at a certain depth (Figure 2). As a result of progressive sinkholes, e.g., when further rock mass movements occur and the void filling starts to migrate downwards ($G > T_w$), the reinforcement under the weight of the pressurized embankment soil elongates from below and takes the form of a stretched membrane with a deflection d . The deflection of the taut diaphragm d is obviously smaller than the deflection of the terrain surface loaded with the load q .

Calculations for geosynthetic reinforcement carried out by the limit state method usually give results for tensile strength at the level of several hundred (or even over a thousand) kilonewtons per meter. This is a very strong geosynthetic reinforcement, rarely used in standard geosynthetic solutions, but the specifics of the case described are exceptional. Of course, if the tensile strength value is very high, several layers of geosynthetic reinforcements with lower strengths may be considered. Geosynthetics made of aramid or polyvinyl alcohol, with very low elongations, are used for such applications. Examples of parameters of such used geosynthetics are presented in Table 1.

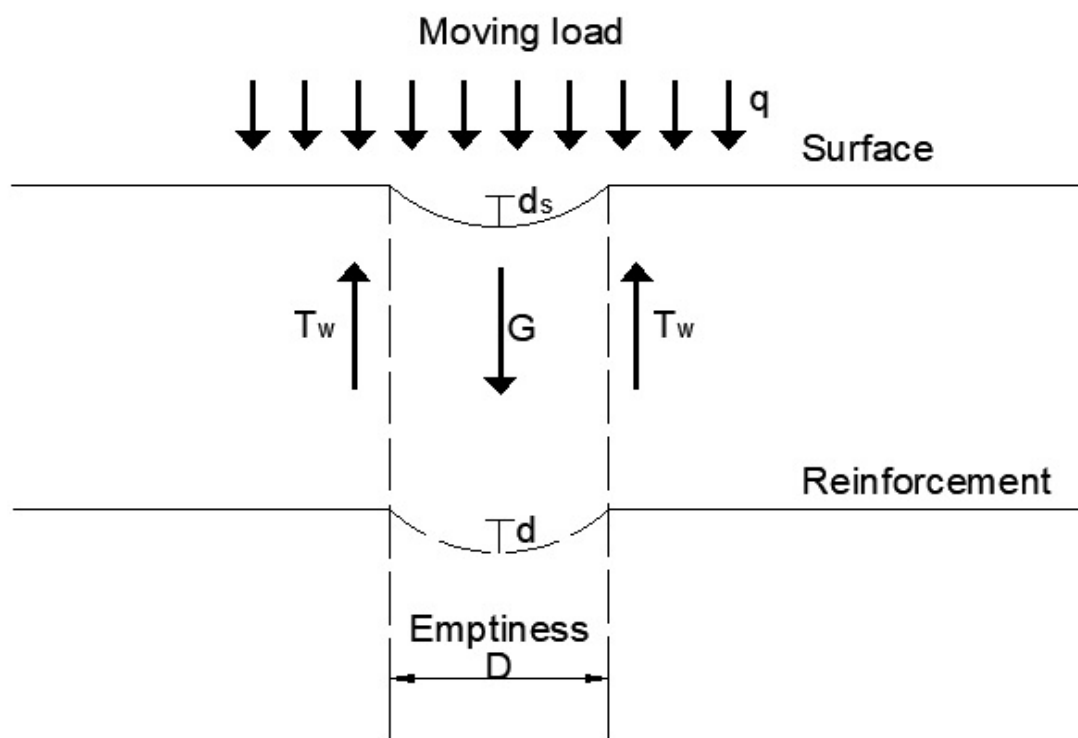


Figure 2. RAFAEL model-sketch. D —sinkhole diameter, d —diaphragm deflection, d_s —road surface deflection, q —load, T_w —sidewall friction force, G —ground weight Adapted from [38].

Table 1. List of exemplary parameters of the applied geosynthetics.

Aramid Geogrid (e.g., Fortrac [®] R 1200/100-30 AMT, HUESKER Synthetic GmbH, Gescher, Germany)	Polyvinyl Alcohol Geogrid (e.g., Fortrac [®] R 830/100-30 MT, HUESKER Synthetic GmbH, Gescher, Germany)
Short-term tensile strength $\geq 1200/100$ kN/m Elongation at maximum load $\leq 3.5/6\%$ Mesh size 30/30 mm Aramid/PVA polymer	Short-term tensile strength $\geq 830/100$ kN/m Elongation at maximum load $\leq 6/6\%$ Mesh size 30/30 mm PVA/PVA polymer

2.1.8. Monitoring

Having obtained the required parameters of the geosynthetic reinforcement as a result of numerical analyses (strength, elongation, load capacity utilization of the reinforcement), it is possible to proceed to the specification of the structure monitoring system. So far, in engineering practice systems, operating in two layers has been used to control and track the stress of geosynthetic reinforcement. The system should enable the nature and area of any deformation to be identified. The first layer, consisting of extension lines, allows for subsidence measurements. The second layer, consisting of elongation sensors installed on the reinforcing geogrid, allows the strain of the geogrid to be measured. In this case, the monitoring system provides precise control and tracking of the strain state of geosynthetic reinforcement and subsidence under the layer of reinforcement. The most common solution is a system based on the use of string sensors. Exemplary pictures of the installed two monitoring layers are presented in Figures 3 and 4. Figure 3 shows elongation lines crossing at specific intervals throughout the monitored area. They are connected to the collecting wells and there they are terminated with sensors that measure the elongations of the lines. Settlement of the ground causes the elongation of two specific lines that intersect with each other, and the appropriate mathematical algorithm calculates the subsidence and its value. Figure 4 shows the strain sensors permanently installed on the reinforcing geogrid. They are encased in a steel, durable cover, which allows the sensor to move freely during geogrid

deformation and during deformation of the subsoil. Both systems are compatible with each other.

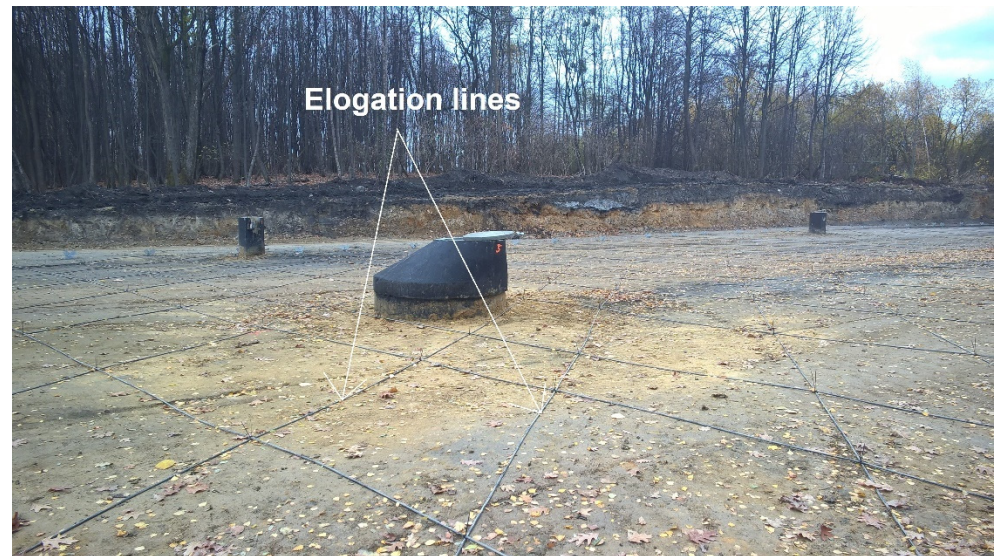


Figure 3. First monitoring layer, measurement of subsidence through elongation links mounted to string sensors—Ruda Śląska, N–S route, Poland 2018 (example of monitoring application).



Figure 4. Second monitoring layer, measurement of elongation in geosynthetic reinforcement—Ruda Śląska, N–S route, Poland 2018 (example of monitoring application).

2.2. Geopolymers

2.2.1. Geopolymers—Properties and Application

Geopolymers are amorphous aluminosilicate materials that are synthesized in a highly alkaline environment at temperatures up to 100 °C. These materials consist of long-chain copolymers of sand and aluminate and metal cations: sodium, potassium, lithium, or calcium, which are used to stabilize these compounds [41]. Origin names are discussed in more detail in the article [41].

Geopolymers are very interesting materials; the greatest interest in them comes from the construction industry [42]. This material has become a good additive to cements—even replacing them in some cases. Geopolymers are added to cements to form injection suspensions. In [43], the authors described conducted tests, in which they combined Portland

cement with geopolymers. The addition of geopolymer substances resulted in a significant liquefaction of the substance and an increase in its material parameters, which had a beneficial effect on soil sealing.

The environmental aspect is why geopolymers began to replace cement. The production of cement introduces very large quantities of CO₂ into the atmosphere. Portland cement production takes place at very high temperatures (1400 °C–1500 °C), with significant amounts of carbon dioxide and nitrogen oxide being emitted into the atmosphere. The production of cement has increased each year, and with it, its impact on the environment. This phenomenon is described in detail by Król (2013, 2015) and Blaszczyński (2010, 2015) [44–46]. According to estimates, the synthesis of geopolymers consumes about 2–3 times less energy than the production of Portland cement and produces 4 to 8 times less CO₂ [47]. The issue of environmental protection is an important aspect that drives the continuous development of geopolymers.

Geopolymer materials, in addition to being environmentally friendly, have gained worldwide popularity due to their other advantages as well, such as:

- High compressive and bending strengths;
- High acid resistance;
- High frost resistance;
- High thermal resistance (geopolymers do not lose their properties at temperatures up to 800 °C);
- Low porosity;
- Fast onset of setting times (compared to that of concrete);
- High degree of adhesion of geopolymers with steel;
- Synthesis of geopolymers consume less energy than, e.g., Portland cement, and release less CO₂ into the atmosphere;
- Water-resistant material; service life of the material reaches up to approximately 100 years;
- Minimal environmental impacts;
- Material reaches 90% of its strength in just 30–90 s;
- 5–30 times expansion of the material;
- Expansion pressure reaches up to 10,000 kPa;
- Material application temperature ranges from –15 °C to 60 °C;
- Geopolymer material is about 10% of the mass of concrete.

2.2.2. Application of Geopolymers for Soil Reinforcement and Rectification of Buildings

An innovative method that has also found its application in the rectification of buildings involves the injection of geopolymer materials into the soil, to raise it to a suitable level. This method is a simple, effective alternative to traditional solutions (the use of lifts and piles). One of the companies that specializes in the stabilization and reinforcement of soil by using geopolymer materials has solutions available all over the world, including in Poland. On the company's website [48], and in its advertising materials, they describe the behavior and properties of geopolymer materials and the process of injecting the material into the rock mass in detail.

Geopolymer materials improve the bearing capacity of the subsoil by filling voids, raising and leveling subsoils and foundations, and sealing and improving resistance to dynamic loads. In addition, the expansion force results in soil compaction and increased stresses in the subsoil.

The application of geopolymer material injections can be divided into two categories: surface and deep consolidation. In surface consolidation, the geopolymer material is injected into the area directly below the structure, filling the voids between the foundation and the underlying soil. Deep consolidation applies to soils that require reinforcement at greater depths and involves increasing the density of the soil.

The geopolymer material, after being injected into the soil, moves and increases its volume both horizontally and vertically. When the material gets into the voids, it begins to

swell, and in the final stage, it changes from a liquid to a solid state. Around the injection point (borehole) an affected area is created with a radius of approximately 1 m. Of course, the extent of the area depends on the geopolymer material used, as well as the properties of the soil into which the material is injected (soil type, bearing capacity, and load).

Soils have different properties, so there are many types of geopolymer materials with different chemical compositions to best “adapt” to the needs of the soil. Each geopolymer material has different characteristics, so it can be used in a wider range of soil conditions.

The injection of geopolymer materials into rock mass is carried out by one of the contractors, in two ways: the extraction method and the multitubular method (Figure 5).

Methods of injecting geopolymers into rock mass

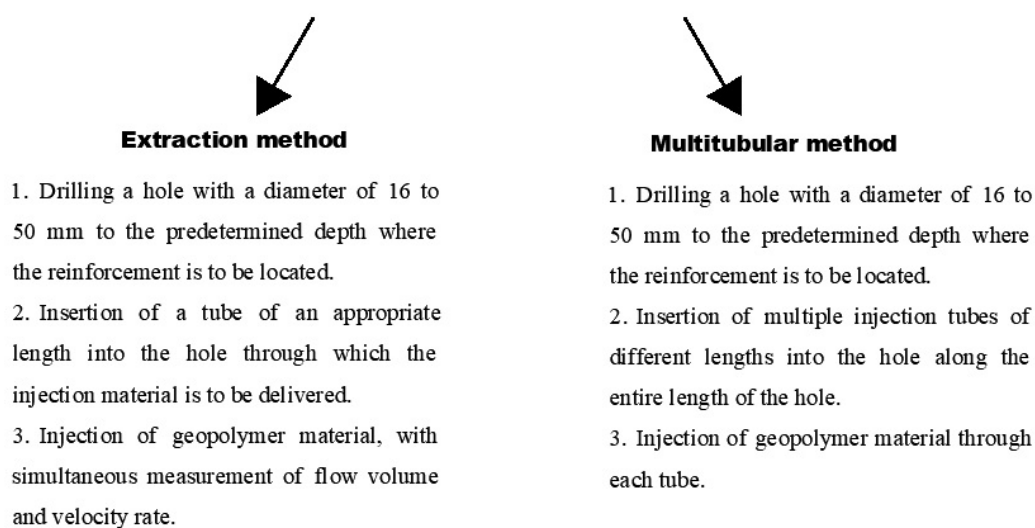


Figure 5. Methods of injecting geopolymer materials. Adapted from [48].

One example of the use of geopolymers for soil reinforcement involves implementation at the National Gallery in Ireland, as part of its refurbishment; it was decided that the soils underlying 28 meters of walling did not possess sufficient strength to safely transfer the proposed loading conditions of 80, 229, 272, and 330 kN/m², respectively. The design and workmanship were prepared by Uretek [49]. In the proposed solution, Uretek specified that the geopolymer injection be carried out, after reviewing the field test report provided by the client and taking into account the maximum load of 330 kN/m² (along with the appropriate dimensions of the foundation)/Uretek determined that the geopolymer injections should take place at a maximum depth of 2.5 m below the ground level. The conducted tests allowed for the conclusion that soil below this depth were capable of safely carrying the appropriate load. After the work was complete, Uretek conducted dynamic probe testing to verify the works.

3. Research

The research area is located in the Upper Silesian Coal Basin and is situated within the administrative borders of city G—Figure 6. The area has been subjected to intensive mining exploitations for many years; due to the unfavorable geological conditions on the surface, linear discontinuous deformations were created on the land surface.

3.1. Methodology

Linear discontinuous deformations of the surface type result from the formation of fractures and slippage of the near-surface soil layer, which is most frequently subjected to continuous deformations due to underground mining excavations [6,7,10,50–52].

Kwiatk (2003) [50], analyzing the impact of horizontal loosening of near-surface layers of soil, stated that the cause of the formation of discontinuities is from bringing

the near-surface layer of the rock mass made of soil to the state of limit equilibrium, as a result of which, slippage surfaces may appear, or, in the cases of horizontal loosening of the layer with cohesion $c \neq 0$, vertical fractures separating soil masses that continue to move as non-deformable masses. The location of the discontinuity surface is determined by accidental factors, such as local strength reduction.

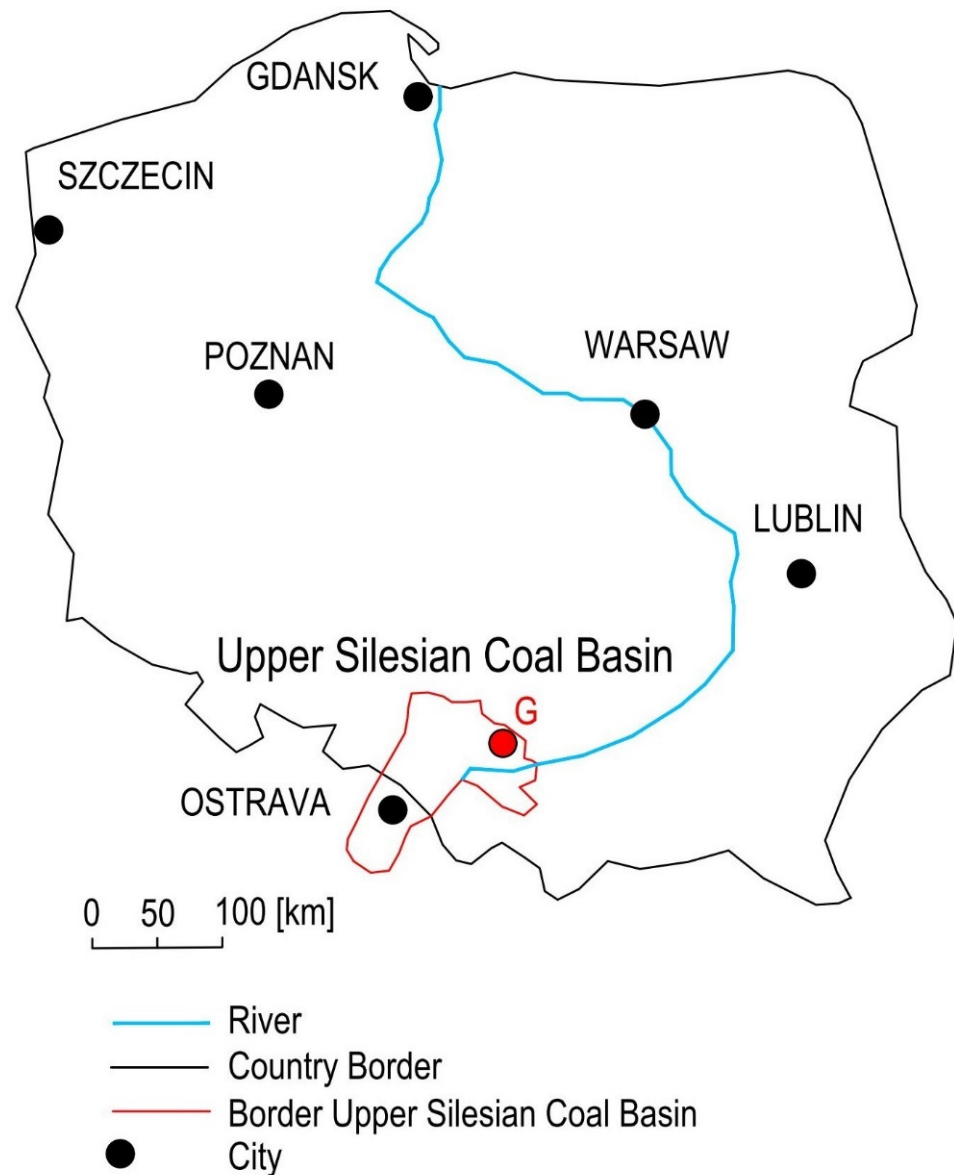


Figure 6. Location of the research area on the map of Poland.

As observed from many years of research and studies [10,50]—geological factors, mainly tectonic factors (outcrops of Carboniferous faults) [52], and widely understood mining factors, have main roles in the creation of linear discontinuous deformations of surfaces.

According to Kratzsch (1983) [1] (Figure 7) and Tyrała (2013) [52], in the area of an outcrop of the fault zone, anomalies in the profiles of subsidence troughs and linear discontinuous deformations may occur. According to Kratzsch (1983) [1], these can take the form of flexures or systems of smaller steps. According to Tyrała (2013) [52], they may cause discontinuous deformations and disturbances of the subsidence trough profile, including elongation or shortening of the trough profile.

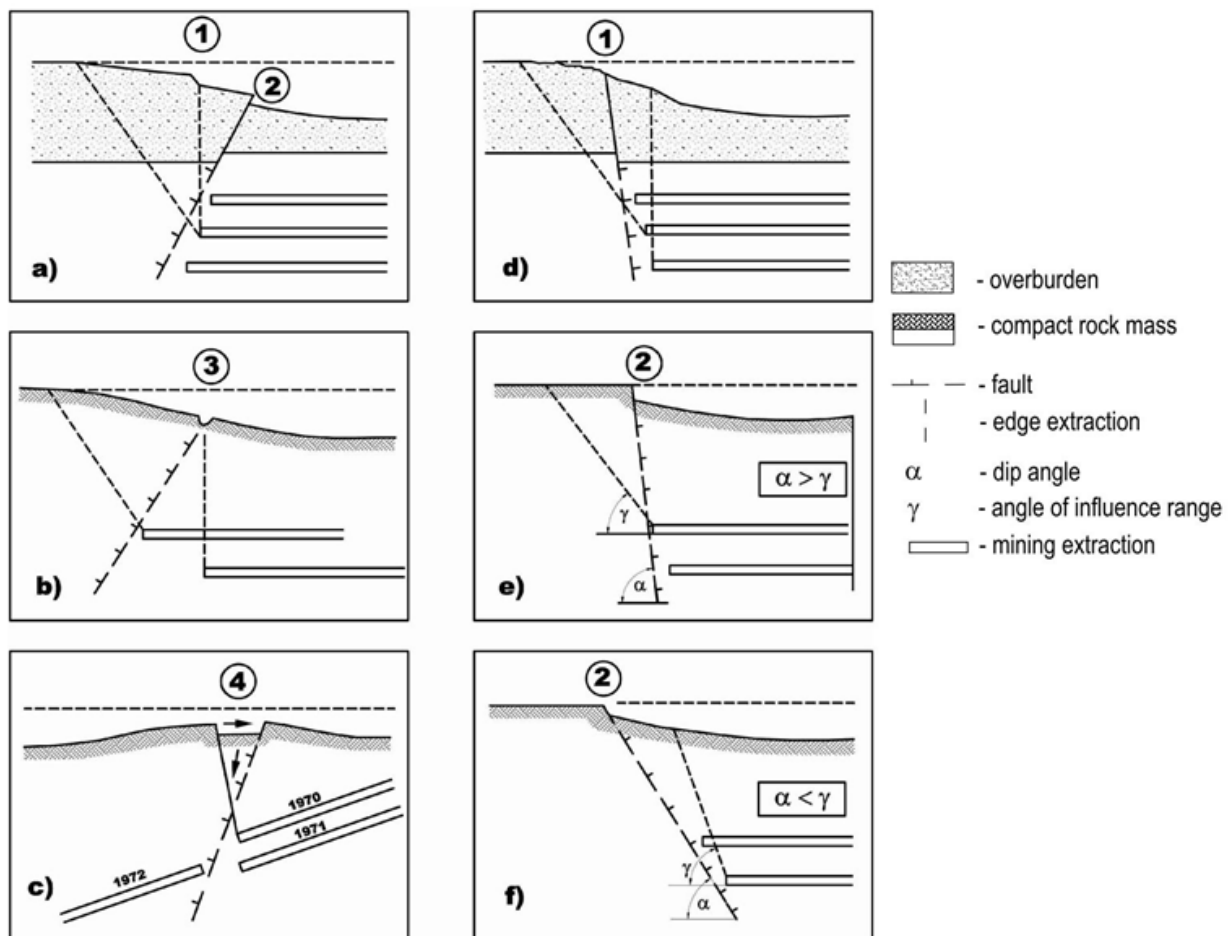


Figure 7. Anomalies of subsidence trough profiles due to fault activation: “(a)” 1—flexures or system of minor steps; 2—ground step; “(b)” 3—fissures; “(c)” 4—graben; “(d)” 1—flexures or system of minor steps; “(e)” 2—ground step $\alpha > \gamma$; “(f)” 2—ground step $\alpha < \gamma$. Adapted from [1].

According to the research conducted by Chudek et al. (1988) [4] (Figure 8), the area threatened by discontinuous deformations in the area of the fault outcrop may be determined by the relation presented below (4):

$$S = 1.2 \cdot h_n \cdot \text{ctg} \alpha \quad (4)$$

where:

S —width of the zone threatened by occurrence of discontinuous deformations, m;

h_n —thickness of the overburden, m;

α —angle of repose of the overburden layers, usually 34° – 43° , degrees.

Linear discontinuous deformations [6,7,10,50–52] may appear above the quickly progressing exploitation front with caving, especially to one common edge, as well as a result of repetitive stoppages of the extraction process (e.g., weekends). They occur in the marginal external parts of subsidence troughs and in the areas of protective pillars established for the protection of main underground workings: shafts, cross-cuts, and cross-headings, as well as in the vicinity of the boundaries of mining areas.

One of the main causes of their formations involves tensile strain zones of large values caused by mining exploitation [6,7,10,50–52].

Kowalski (2015) [10] indicates that these are strains of the order of category V of the mining area (according to the Polish classification of mining areas). At such a level of strain values, primary linear deformations are formed on the surface, while activated deformations occur at tensile strains reaching approximately 2 mm/m and these discontinuities are usually of secondary (repetitive) nature.

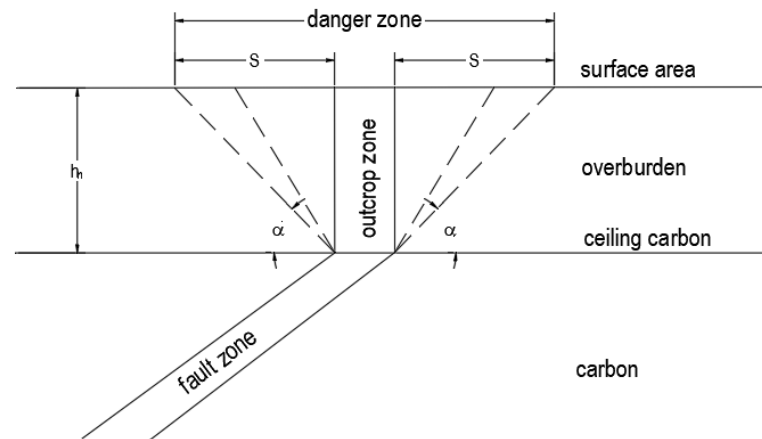


Figure 8. Width of the zone threatened by occurrence of discontinuous deformations in the area of fault outcrops. Adapted from [4].

According to the research conducted by Kwiatek (2003) [50] on the impact of horizontal loosening of loose and cohesive soils, in the aspect of formation of small discontinuity deformations, the limit state for loose soil, under the impact of horizontal tensile strains, begins in the near-surface layer of soil and progresses deep into the rock mass at a strain equal to 2 mm/m and covers a soil layer approximately 5 cm thick, and at a strain of 4 mm/m–10 cm thick. For cohesive soil, the limit state occurs at tensile strains of 3 to 9 mm/m, depending on the type of soil and its vertical load.

3.2. Description of the Research Area

The evaluation of the possibility of restoring the utility value of the near-surface rock mass layer, by means of geopolymer injection and geosynthetics, was carried out for the area where linear discontinuous deformations were identified in the past.

In the area of the analyzed property, five discontinuous deformations were found. Deformation number 5 presents the properties of a typical discontinuity in terms of breaking and displacement of the near-surface rock mass layer, whereas deformation nos. 1 to 4 show intermediate features between flexure and typical discontinuity. It means that the displacement of the near-surface layer occurred, but the breaking did not occur or occurred fragmentarily—Figures 9 and 10. The form of occurrence of these deformations is probably connected with the geological structure of the overburden, with a large share of plastic clays, loams, and clay stones. The time of occurrence of the discontinuities is not precisely known.



Figure 9. Discontinuity number 3—view to the east from the building; h —the height of the fault drop.

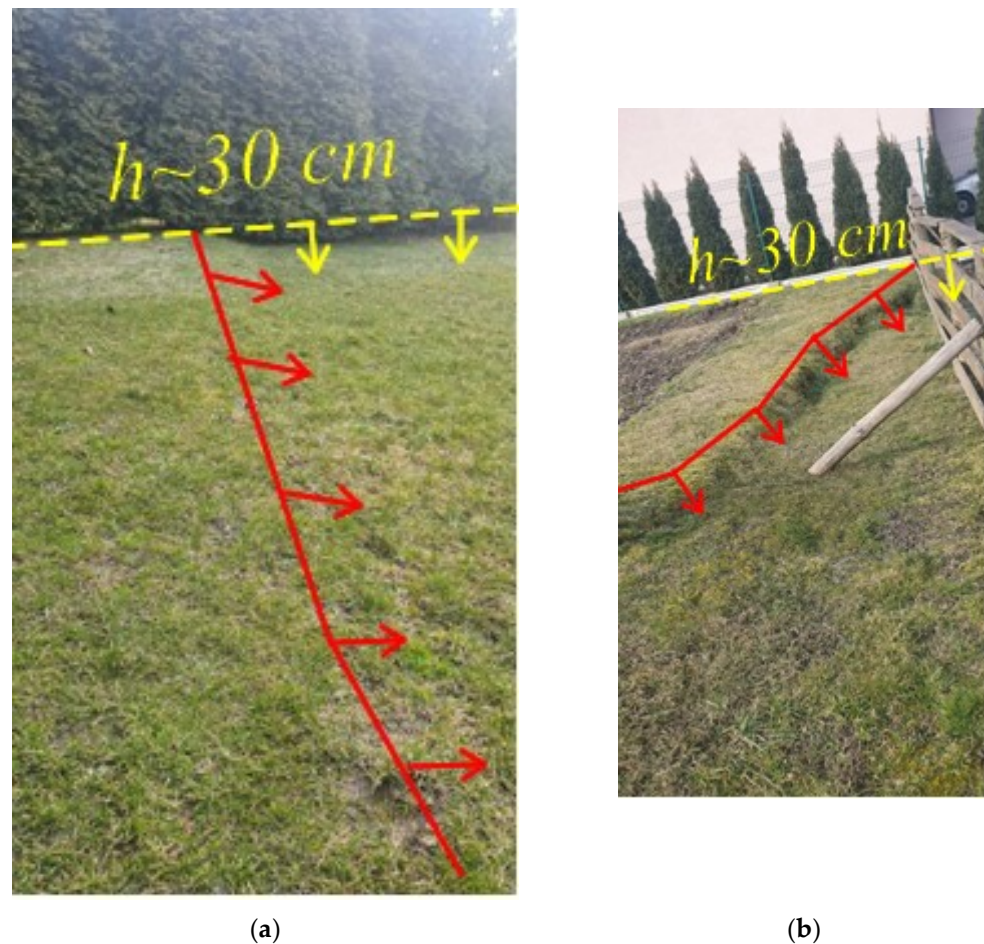


Figure 10. The view of discontinuity—“(a)” number 3; “(b)” number 5, h —the height of the fault throw.

3.3. Geological Structure of the Rock Mass, Tectonics, Mining Exploitation

The geological structure of the rock mass was recognized on the basis of the map of Quaternary and Tertiary formations and the profile of borehole A, situated approximately 359 m to the north of the studied area—Figure 11.

The rock mass in the studied area is made of an overburden and Carboniferous beds. In stratigraphic terms, the overburden is formed by Quaternary and Tertiary formations. The thickness of the Quaternary layer directly under the site is approximately 23 m. These formations consist of soil, clay, and sand. The thickness of the Tertiary beneath the site is approximately 170 m. It consists mainly of loams and clay stones.

Carboniferous formations include the “Orzesze” beds (seams of group 300, according to the Polish classification of Carboniferous layers) and the “Ruda” beds (seams of group 400). An incomplete profile of the “Orzesze” beds was identified in the study area. Seams 352, 355, 357, 358, 359, and 361 occur in this area. The “Orzesze” beds consist mainly of clay stones and shales, but sandstones are also present. The “Ruda” beds occur from a depth of approximately 660 m. They are formed mainly as claystones, mudstones, coal beds, and coal shales. Coal seams 401/1, 401/2, 405/1, and 405/3 are present here.

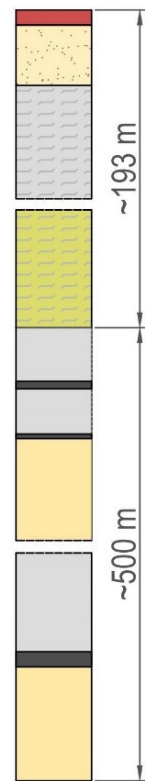
Three tectonic faults were found in the direct vicinity of the study area. The fault outcrops run nearly latitudinal. The exact course of these dislocations is shown in Figure 12.

Fault I runs at a distance of about 105 m south of the studied area. At a depth of approximately 250 m, there is a branching of this fault into two separate parts. Both throw rock mass beds to the north by height—the first approximately 17 m and the second approximately 13–25 m. The angle of dip of the fault surface is approximately 50° for

branch 1 and 61° for branch 2. The surface of these faults is located directly under the object at the depth of approximately 850 m.

Lithological profile of borehole X

+256.0 m a.s.l



Quaternary

- soil
- sand
- clay

Tertiary

- loam
- loam

Carboniferous formations

- slate
- coal
- sandstone

Figure 11. Lithological profile of borehole X.

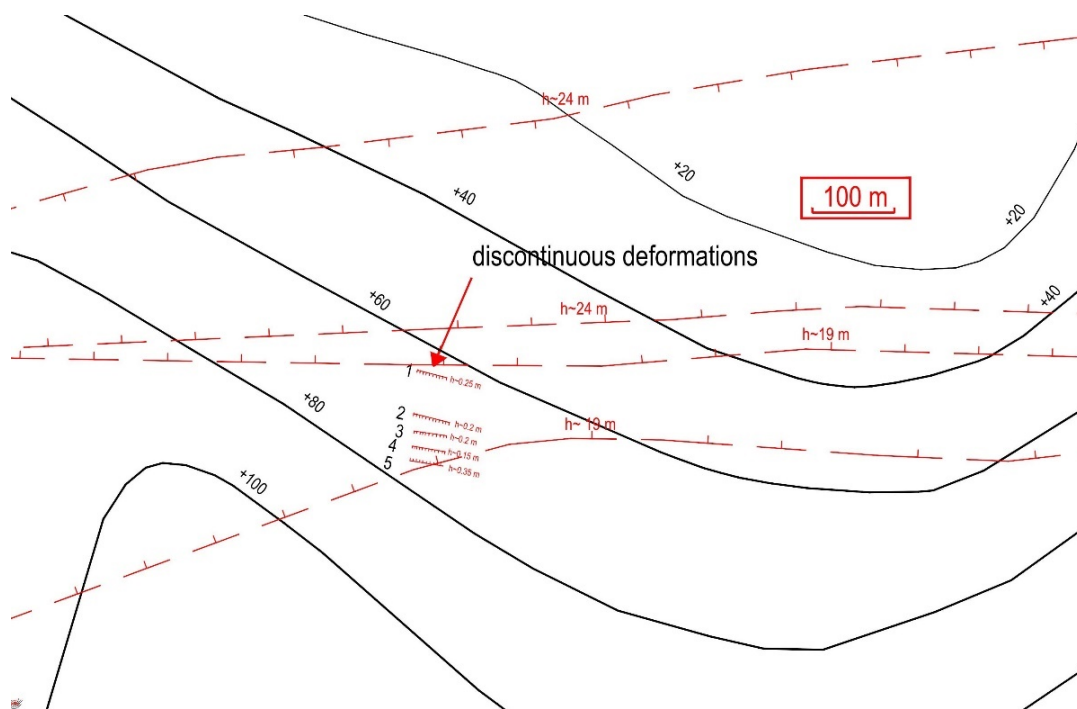


Figure 12. Map of the roof of Carboniferous layers with the location of linear discontinuous deformations.

Fault II runs directly under the studied area and throws rock mass beds by the height of approximately 19 m towards the north. Its angle of dip is approximately 124° . The surface of this fault is located directly under the object at the depth of approximately 290 m. Due to the identified discontinuity passing under the object, it cannot be excluded that the outcrop of this fault on the roof of Carboniferous layers is located closer to the object than the map indicates.

Fault III, which throws the rock mass beds by about 25 m towards the north, runs approximately 51 m north of the studied area. The angle of dip of the fault surface is approximately 125° . The surface of this fault is located directly under the object at the depth of approximately 630 m.

The roof of the Carboniferous layers is located at the height of approximately +57 m above sea level. The rock mass dips towards the south-east, at an angle exceeding 10° .

The mining exploitation was carried out by a longwall system with caving in seven hard coal seams: 352, 355, 357, 358, 359, 361, 401/1. A sketch illustrating all mining exploitation, carried out together with locations of discontinuous deformations, is presented in Figure 13.

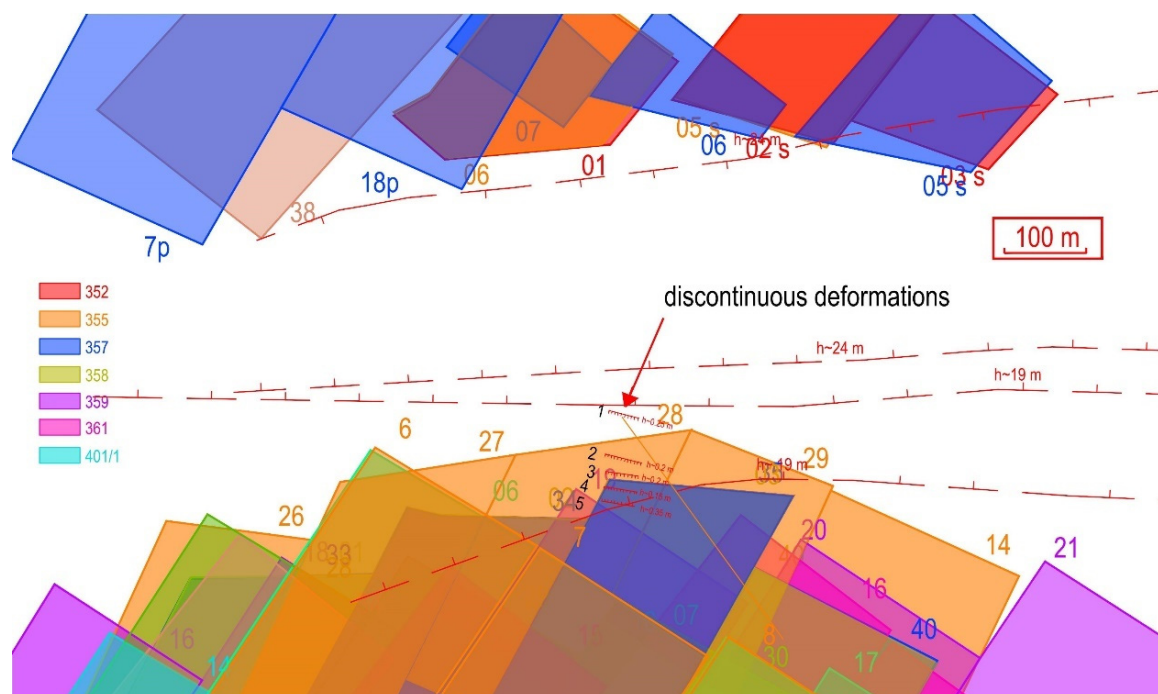


Figure 13. Sketch illustrating all mining exploitations in the study area.

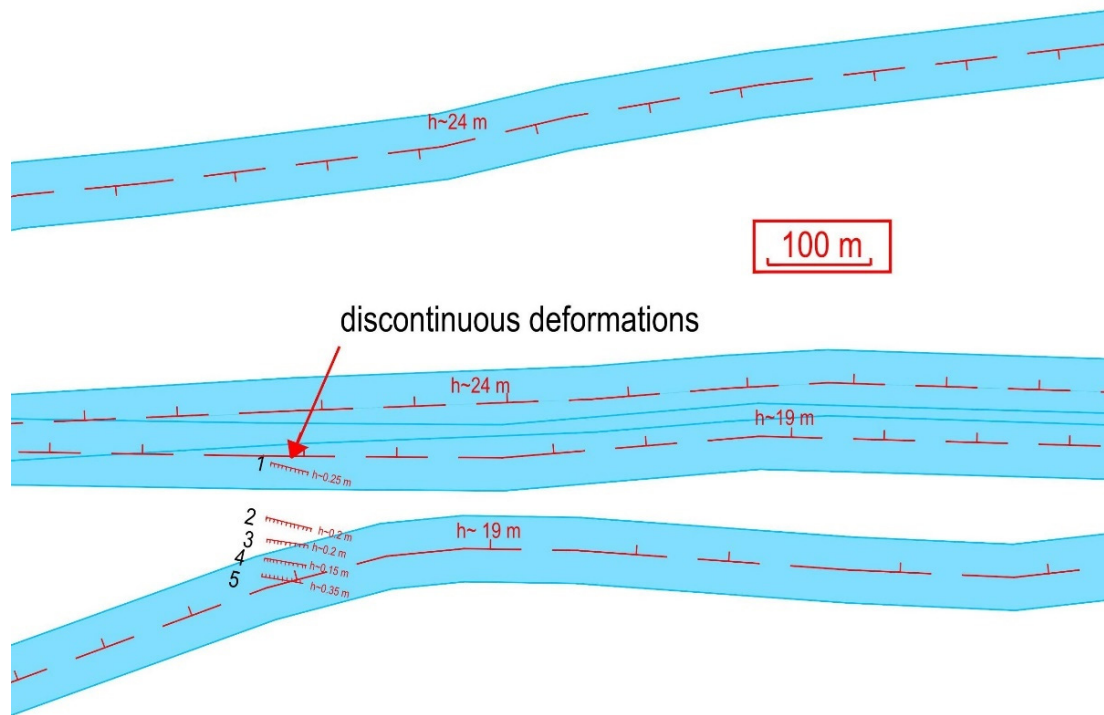
3.4. Causes of the Formation of Discontinuities

In order to determine the causes of the linear discontinuous deformations found in the study area, an analysis of the geological and mining conditions was carried out, which led to the determination of possible causes of the discontinuities formation. These are:

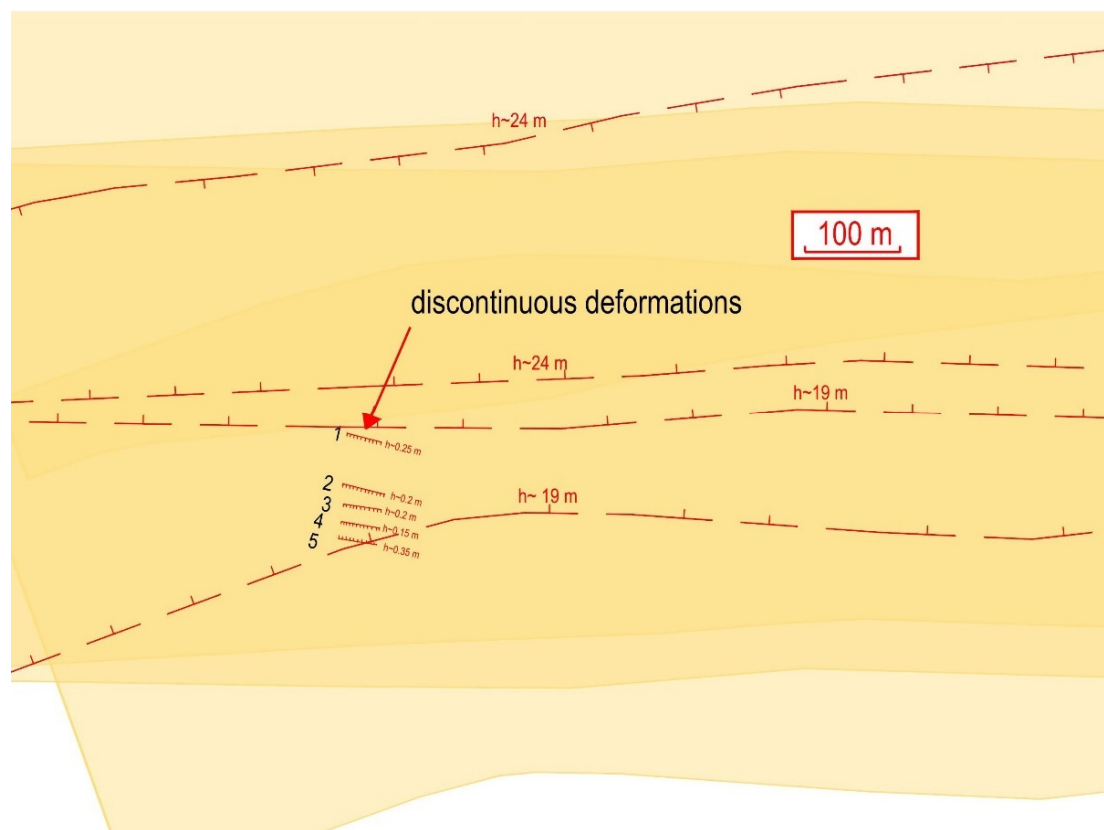
- (1) Outcrops of tectonic faults on the roof of the Carboniferous layers.
- (2) Tensile strain zones as a result of mining exploitation.

Having determined the threatened zone in the area of fault outcrops (4) by means of relations, it was decided to check whether the studied area was within the range of this zone. Calculations of the width of the area at risk of discontinuous deformation in the area of the fault outcrop (S) were carried out for two variants:

- (1) Value “ S_1 ” was calculated for data: $H = 23$ m—Figure 14a, where H is the thickness of the Quaternary loose formations. Only loose overburden was taken into account.
- (2) Value “ S_2 ” was calculated for data: $H = 191$ m—Figure 14b, where H is the thickness of formations overlying the Carboniferous formations.



(a)



(b)

Figure 14. The zone threatened by occurrence of discontinuous deformations in the area of fault outcrops (a) S_1 , (b) S_2 calculated from Equation (4).

In both variants, the value of the angle of repose of overburden layers equal to 40° was assumed. It was determined on the basis of experience from other areas with similar geological conditions. In view of the results of the calculations, the threatened zone in the area of the fault was approximately $S_1 = 32.8$ m, $S_2 = 272.7$ m. It means that, in variant 1, the threatened zone covered the property on the northern side—discontinuity number 1, and on the southern side—discontinuity nos. 3, 4, 5—Figure 14a. In variant 2 the threatened zone covers the whole analyzed property—Figure 14b.

Calculations of maximum horizontal strain were carried out by simulating the progress of the exploitation for the whole exploited area, in order to fully illustrate how the mining excavation affected the surface in the form of tensile strain. A simulation interval of 10 days was assumed. Calculations were performed for ϵ_{\max} [2] without taking into account relaxation phenomena, and for $\epsilon_{\max R}$ [53], accounting for the relaxation simulating the decrease in deformation over time. The results are presented in Figure 15. It should be noted that, in performing the calculations, the authors are fully aware that the summation of the values of horizontal strains in the long time intervals is problematic and the opinions are divided on the method of the summation [54]. However, for the prognosis concerning the determination of the course of the tensile strains, it was deemed useful in assessing the possibility of the occurrence of the limit equilibrium state of the near-surface rock mass layer.

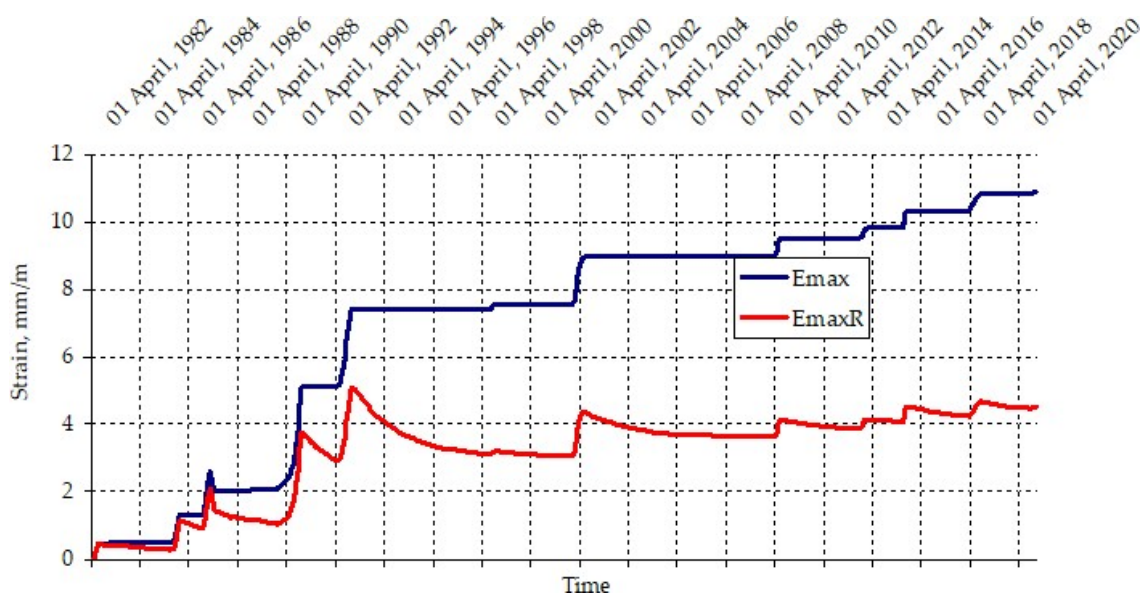


Figure 15. The course of the maximum horizontal strain with consideration of the so-called “relaxation” ($\epsilon_{\max R}$), according to Bialek (2003) [53], and without taking it into account (ϵ_{\max}) [2], with the assumption of the immediate manifestation of impacts.

As seen in Figure 15, the courses of the horizontal strain for ϵ_{\max} and $\epsilon_{\max R}$ are similar to each other, but different in value. In both cases, it is also evident that the surface was subjected to tensile strain during the whole exploitation period. The values of ϵ_{\max} tensile strain were within the range of category V of the mining area. In the case of $\epsilon_{\max R}$, the maximum strain accounting for relaxation, the values of the tensile strain reached category III. The values of the strain and the tensile characters of these deformations have a fundamental impact on the process of formation of discontinuity nos. 1–5 in the studied area.

Based on the obtained analyses and calculation results, it can be assumed that the main reasons for the occurrence of discontinuous deformations on the surface is the tensile strain caused by underground mining and the existence of tectonic structures inside the rock mass. The results presented above come from computer simulations, which should be treated as approximations of the real deformation state. However, no observations of

the terrain surfaces were carried out in the analyzed region; therefore, the results of this re-forecast is the only source of information on the surface deformation state.

3.5. Concept of Site Protection

Considering the fact that the ground deformations were caused by tensile strain, the restoration of the utility value of the near-surface rock mass layer should be carried out by constructing a protective structure that will work in conditions of strain. In this case, this function can be performed by reinforced earthwork founded at the ground level. The calculated maximum horizontal strain (Figure 15) is within the range of ~4.3–11 mm/m and, therefore, the protective structure must feature a very low strain. One of the most effective ways of reinforcing earthworks is the use of geosynthetics, characterized by both high tensile strength and low strain. Appropriately selected geosynthetics exhibit good adhesion with the backfill soil, thus creating a very good reinforcing composite.

Reinforced geosynthetics with the lowest strains are made of aramid. The value of strain in this type of geosynthetic, verified in tests carried out in testing machines, is approximately 3%. This is the strain at maximum load and it is measured in accordance with EN ISO 10,319 [30]. The test lasts approximately 20 s and is carried out under laboratory conditions (i.e., in air at 20 °C, no contact with the ground or varying weather conditions). It should be noted that this is a short-term measurement and it is not carried out under real-natural conditions. In order to get closer to natural conditions, the reinforcement must be dimensioned according to the limit state method [31,32,55], taking into account, i.e., the material and safety factors (see point 2.2.).

In the reinforcement structure in question, the geosynthetic made of aramid should be arranged in two directions: parallel and perpendicular to the measured tensile strain. The friction angle at the junction between the geosynthetic and the backfill soil must provide the required anchorage beyond the protection zone, adequately, for the required tensile strength. The best results are obtained by creating a composite, geogrid of crushed, fractionated aggregate. In engineering practices, it is customary to put at least four layers of geosynthetics, two in each direction, separated by a compactable aggregate layer. The practice is to put and compact aggregate layers with a maximum vertical spacing of 25 cm. Additionally, a bearing layer of natural aggregate of even grain size (e.g., gravel) may be applied below, allowing for initial dissipation of stresses arising in the reinforcing structure. From a technological point of view, in order to facilitate the work on the bearing layer, it is possible to install this layer in a geogrid.

When designing a protective structure, recommendations, methods, and formulae from the literature can be used. The most widely described design guidelines and the most used mathematical formulas and dependencies, as well as practical advice, can be found in the EBGeo 2010 [35]. Using the EBGeo, it is possible to tackle the issues described in this paper. However, it is worth taking into account the examples of structures that have been constructed and used for many years, which provide an idea of the effectiveness of the adopted methods of reinforcement. Of course, it should be kept in mind that each case should be considered individually, and the project should be supported with the necessary analyses and mathematical calculations, in accordance with the literature mentioned in this work. An example may be the A1 Pyrzowice–Piekary motorway in Poland, which has been in operation for over 10 years (Figure 16), or the Gröbers junction in Germany, which has operated for more than 20 years (Figure 17), and is reinforced with aramid geogrids.

The construction proposed above should also be monitored due to the strain on the geosynthetic reinforcement. For this purpose, string sensors installed on the geogrids are proposed to measure the elongation value of the geogrid. In such a system, it is possible to define limit conditions, alarm, and failure states, and to establish repair procedures in the situation of excessive strain on the structure.

The described system will perform its function properly if the rock mass under the reinforcing structure is free of cracks, voids, and other discontinuous deformations. For this purpose, geopolymer material is injected into the openings. Adequately selected material

fills the voids, increasing the strength values of the soil. The described system will perform its function properly if the rock mass under the reinforcing structure is free of cracks, voids, and other discontinuous deformations. For this purpose, geopolymer material is injected into the openings. Adequately selected material fills the voids, increasing the strength values of the soil. Geopolymer injection is the subject of further research by the authors.



Figure 16. Reinforcement with aramid geosynthetics at the foundation level of the A1 Pyrzowice–Piekary 2011 motorway (shallow mining exploitation and mining faults).



Figure 17. Reinforcement with aramid geosynthetics at the foundation level of the Gröbers junction 2001 railway embankment (sinkholes up to 4 m in diameter were present).

According to the paper [56], the proposed solution may be a geopolymer of the following specifications: fly ash (600 kg/m^3), NaOH (85.7 kg/m^3), Na_2SiO_4 (214.3 kg/m^3), natural sand (279.8 kg/m^3), A-LWA artificial aggregate (701.6 kg/m^3), superplasticizer (12 kg/m^3). The ratio of the alkaline activator to solid (fly ash) should be 0.5 and the alkaline activator should be a mixture of an NaOH solution and Na_2SiO_4 ready solution. The total content of the alkaline activator should be 300 kg/m^3 and the ratio of sodium hydroxide to sodium silicate can be determined as 1:2.5.

4. Summary

This paper presents a case study of surface damage caused by linear discontinuous deformations, with origins related to intensive mining exploitation in unfavorable geological conditions (the presence of a tectonic fault zone). It presents a proposal for protection of the damaged area using geosynthetics and geopolymers. These materials are modern solutions used for protecting surfaces subjected to factors related to mining exploitation.

Based on the analysis of geological conditions, it can be concluded that rock mass is made of Quaternary, Tertiary, and Carboniferous formations (the Orzesze and Ruda beds). The Carboniferous beds are traversed by latitudinal faults where surface threatened zones were established in the study and the impact of mining exploitations of seven hard coal seams in the studied area were simulated. As a result of the calculations, values of horizontal strain, increasing with the extraction of successive longwalls up to 11 mm/m, were obtained.

The category of the “mining area”, depending on the interpretation of the horizontal strain (including the relaxation (or not) of the horizontal strain), ranged from III (with relaxation) to V (without relaxation). Such high values of the terrain category and the occurrence of tectonic faults in Carboniferous beds were found to be the main causes of linear discontinuous deformations, which is confirmed by studies conducted in this field to date [6,7,9,10].

To protect the surface from damage, a reinforced structure made of aramid laid in two directions—parallel and perpendicular to the calculated tensile strain—was proposed. In addition, we recommend using a geopolymer material injected through holes to remove gaps and voids from the rock mass.

5. Conclusions

In the introduction, we noted that, so far, no joint protection in the form of geogrids and geopolymer injections has been used to protect the terrain surface. The solution may initially seem costly, but the examples of damage to national road number 44 [6] makes it possible to quickly solve the problem by injecting geopolymers, with the initial protection with geogrids, which was made during the road renovation and did not fulfill its task. The proposed solution should be tested in practice in an area where a planned mining extraction will be conducted in difficult geological conditions (presence of tectonic faults). One significant limitation surrounding the solution may be the cost of making a double protection system. In further perspectives, it should be possible to conduct research on the possibility of rectifying buildings and strengthening the ground damaged by underground mining operations.

Author Contributions: Conceptualization, D.P.; methodology, D.P., K.S., M.P.; software, K.S.; validation, D.P., K.S.; formal analysis, D.P., K.S., M.K., M.P.; investigation, D.P., K.S., M.P.; resources, D.P., M.K.; data curation, K.S., M.P.; writing—original draft preparation, D.P., K.S., M.K., M.P.; writing—review and editing, M.K., K.S.; visualization, D.P., K.S., M.K., M.P.; supervision, D.P., K.S.; project administration, D.P., K.S., M.K. All authors have read and agreed to the published version of the manuscript.

Funding: The publication was financed under the Excellence Initiative-Research University program at the Silesian University of Technology, 2020–2021 (grant number 06/040/SDU/10-22-01).

Institutional Review Board Statement: Not applicable.

Informed Consent Statement: Not applicable.

Data Availability Statement: The data presented in this study are available on request from corresponding author.

Acknowledgments: The authors are thankful to the Silesian University of Technology, Poland, for providing all of the facilities to perform the research work.

Conflicts of Interest: The authors declare no conflict of interest.

References

1. Kratzsch, H. *Mining Subsidence Engineering*; Springer: Berlin/Heidelberg, Germany; New York, NY, USA, 1983; p. 543.
2. Knothe, S. *Forecasting the Impact of Mining Exploitations*; Publishing House “Slask”: Katowice, Poland, 1984; p. 122.
3. Whittaaker, B.N.; Reddish, D.J. *Subsidence. Occurrence, Prediction and Control*; Elsevier: New York, NY, USA, 1989; p. 528.
4. Chudek, M.; Janusz, W.; Zych, J. Study on diagnosis and prognosis of the formation of discontinuous deformation due to underground mining. *Res. J. Silesian Univ. Technol. Gliw.* **1988**, *141*, 165. (In Polish)

5. Strzałkowski, P. *Zarys Ochrony Terenów Górniczych*; Wydawnictwo Politechniki Śląskiej: Gliwice, Poland, 2010; p. 192.
6. Ściagała, R.; Szafulera, K. Linear discontinuous deformations created on the surface as an effect of underground mining and local geological conditions—Case study. *Bull. Eng. Geol. Environ.* **2019**, *79*, 2059–2068. [[CrossRef](#)]
7. Strzałkowski, P.; Szafulera, K. Occurrence of linear discontinuous deformations in Upper Silesia (Poland) in conditions of intensive mining extraction—Case study. *Energies* **2020**, *13*, 1897. [[CrossRef](#)]
8. Strzałkowski, P.; Ściagała, R.; Szafulera, K.; Kołodziej, K. Surface Deformations Resulting from Abandoned Mining Excavations. *Energies* **2021**, *14*, 2495. [[CrossRef](#)]
9. Kowalski, A.; Jędrzejec, E.; Gruchlik, P. Linear discontinuous deformations of the surface in the Upper Silesian Coal Basin. *Arch. Min. Sci.* **2010**, *55*, 331–346.
10. Kowalski, A. *Deformacje Powierzchni w Górnośląskim Zagłębiu Węglowym*; Główny Instytut Górnictwa: Katowice, Poland, 2015; p. 283.
11. Koerner, R.M. *Designing with Geosynthetics*, 5th ed.; Pearson Prentice-Hall Publ. Co.: Upper Saddle River, NJ, USA, 2005; p. 783.
12. Sarsby, R.W. (Ed.) *Geosynthetics in Civil Engineering*; Woodhead Publishing Ltd.: Cambridge, UK, 2007; p. 295.
13. Koerner, R.M.; Te-Yang, S. The evolution of geosynthetics. *Civ. Eng.* **1997**, *67*, 62–64.
14. Ajdukiewicz, J.; Pilch, M.; Zych, J. Obserwacje i wnioski wynikające z pracy nasypu zbrojonego geosyntetykami na terenie podlegającym dużym wpływom eksploatacji górniczej w Jastrzębiu-Bziu. *Przegląd Komun.* **2013**, *3*, 14–23.
15. Cała, M.; Cieślak, J.; Flisiak, J.; Kowalski, M. Przyczyny awarii nasypu autostrady A4 pomiędzy węzłami „Wirek” i „Batorego” w świetle obliczeń numerycznych. *Nowocz. Bud. Inżynieryjne* **2007**, *1*, 38–44.
16. Kotyrba, A.; Kowalski, A. Linear discontinuous deformation of A4 highway within mining area “Halemba”. *Gospod. Surowcami Miner.* **2009**, *25*, 303–317.
17. Zych, J.; Tondera, M.; Machowski, M. Designing, execution and using stage of highway A4 (E40) based on active geological fault. In Proceedings of the EuroGeo 6, Ljubljana, Slovenia, 25–28 September 2016; pp. 916–926.
18. Grygierek, M. Change in stiffness of pavement layers in the linear discontinuous deformation area. *IOP Conf. Ser. Mater. Sci. Eng.* **2017**, *245*, 42051. [[CrossRef](#)]
19. Chudek, M.; Kleta, H. Zagrożenie obiektów przyszybowych deformacjami nieciągłymi typu liniowego. *Górnictwo Geoinżynieria* **2007**, *31*, 135–140.
20. Miłkowski, A.; Pilecki, Z.; Kłosek, K.; Tondera, M. Autostrada A1 zaprojektowana na “dziurawym” podłożu. Cz. 1. *Mag. Autostrady* **2010**, *3*, 104–112.
21. Miłkowski, A.; Pilecki, Z.; Kłosek, K.; Tondera, M. Autostrada A1 zaprojektowana na “dziurawym” podłożu. Cz. 2. *Mag. Autostrady* **2010**, *5*, 152–160.
22. Kawalec, J.; Grygierek, M.; Koda, E.; Osiński, P. Lessons learned on geosynthetics applications in road structures in Silesia mining region in Poland. *Appl. Sci.* **2019**, *9*, 1122. [[CrossRef](#)]
23. Grygierek, M.; Sternik, K.J. Identification of pavement model parameters in the area of discontinuous surface deformation based on FWD tests. *Int. J. Civ. Eng.* **2020**, *19*, 265–282. [[CrossRef](#)]
24. Juraszek, J.; Gwóźdź-Lasoń, M.; Logoń, D. Fbg strain monitoring of a road structure reinforced with a geosynthetic mattress in cases of subsoil deformation in mining activity areas. *Materials* **2021**, *14*, 1709. [[CrossRef](#)]
25. Tong, L.; Liu, L.; Yu, Q. Highway construction across heavily mined ground and steep topography in southern China. *Bull. Eng. Geol. Environ.* **2013**, *73*, 43–60. [[CrossRef](#)]
26. Tong, L.; Leo, L.; Amatyia, B.; Liu, S. Risk assessment and remediation strategies for highway construction in abandoned coal mine region: Lessons learned from Xuzhou, China. *Bull. Eng. Geol. Environ.* **2015**, *75*, 1045–1066. [[CrossRef](#)]
27. Guo, Q.; Guo, G.; Li, Y.; Wang, L.; Zhao, X. Stability evaluation of an expressway construction site above an abandoned coal mine based on the overlay and index method. *Sustainability* **2019**, *11*, 5163. [[CrossRef](#)]
28. Guo, Q.; Li, Y.; Meng, X.; Guo, G.; Lv, X. Instability risk assessment of expressway construction site above an abandoned goaf: A case study in China. *Environ. Earth Sci.* **2019**, *78*, 588. [[CrossRef](#)]
29. Schwerdt, S. Development of a design method for bridging systems in areas with dolines and sinkholes using geosynthetic reinforcement. *Строительство Архитектура* **2016**, *7*, 132–147. (In German) [[CrossRef](#)]
30. *PN-EN ISO 10319:2010*; (U) Geosyntetyki—Badania Wytrzymałości na Rozciąganie Metodą Szerokich Próbek. The Polish Committee for Standardization: Warsaw, Poland, 2010.
31. *PN-EN 1997-1*; Eurokod 7. Projektowanie Geotechniczne. Część 1. Zasady Ogólne. The Polish Committee for Standardization: Warsaw, Poland, 2010.
32. Wysokiński, L.; Kotlicki, W. *Projektowanie Konstrukcji Oporowych, Stromych Skarp i Nasypów z Gruntu Zbrojonego*; ITB Seria Instrukcje, Wytyczne, Poradniki nr 429: Warsaw, Poland, 2007.
33. *DIN 1054:2010*; Baugrund, Sicherheitsnachweise im Erd- und Grundbau. Deutsches Institut für Normung: Berlin, Germany, 2010.
34. *DIN 4084:2009*; Baugrund, Geländebruchberechnungen. Deutsches Institut für Normung: Berlin, Germany, 2009.
35. Deutsche Gesellschaft für Geotechnik. *Empfehlungen für den Entwurf und die Berechnung von Erdkörpern mit Bewehrungen aus Geokunststoffen EBGE0*; Ernst & Sohn: Berlin, Germany, 2010.
36. *BS 8006:2010*; Code of Practice for Strengthened/Reinforced Soils and Other Fills. BSI: London, UK, 2010.
37. *XP G 38-064:2010*; Utilisation des Géotextiles et Produits Apparentés, Murs Inclínés et Talus Raidis en Sols renforcés Par Nappes Géosynthétiques. AFNOR: Paris, France, 2010.

38. Sobolewski, J.; Ajdukiewicz, J. Geosyntetyki w nasypach komunikacyjnych na terenach zdewastowanych oraz w obszarach zagrożonych deformacjami pogórnictwami, zasady projektowania i przykład zastosowania na autostradzie A1. *Inżynieria Morska Geotech.* **2015**, *5*, 746–756.
39. Papiou, C.; Baraize, E.; Perrier, H. Reinforcement de Plate-Forme autoroutière au-dessus de Cavités Karstiques. In Proceedings of the International Conference Geotextiles Geomembranes-Rencontres 95, Beaune, France, 27–28 September 1995; pp. 93–99.
40. Gourc, J.P.; Villard, P.; Giraud, H. Sinkholes beneath a reinforced earth fill a large-scale motorway and railway experiment. In Proceedings of the Geosynthetics'99: Specifying Geosynthetics and Developing Design Details, Boston, MA, USA, 28–30 April 1999; Volume 2, pp. 833–846.
41. Davidovits, J. Chemistry of geopolymer systems, terminology. In Proceedings of the Geopolymer'99 International Conferences, Saint-Quentin, France, 30 June–2 July 1999.
42. Davidovits, J. *Why the Pharaohs Built the Pyramids with Fake Stones*; Godefroy, J.-C., Ed.; Institut Géopolymère: Paris, France, 2002.
43. Stryczek, S.; Gonet, A.; Wiśniowski, R.; Złotkowski, A. New-generation sealing slurries for borehole injection purposes. *Arch. Min. Sci. Kraków* **2015**, *60*, 931–940. [[CrossRef](#)]
44. Błaszczczyński, T.; Król, M. Durability of Green-Concretes. In Proceedings of the 8th International Conference AMCM 2014, Wrocław, Poland, 16–18 June 2014; pp. 530–540.
45. Błaszczczyński, T.; Król, M. Geopolymers in construction. *Civ. Environ. Eng. Rep.* **2015**, *16*, 25–40.
46. Błaszczczyński, T. Betonowe cuda. In Proceedings of the XXV Ogólnopolskie Warsztaty Pracy Projektanta Konstrukcji, Tom I, Szczyrk, Poland, 10–13 March 2010; pp. 1–41.
47. Król, M.; Błaszczczyński, T. Ekobetonu geopolimerowe. *Mater. Bud.* **2013**, *11*, 23–26.
48. Available online: <https://podnoszenie-posadzek.geobear.pl/> (accessed on 20 November 2021).
49. Bromley, L.; Hadfield, D. *Geotechnical Asset Management: How Structural Engineers Can Exploit Goe-Polymer Injection Technology*; URETEK: Tomball, TX, USA, 2017.
50. Kwiatek, J. *Obiekty Budowlane na Terenach Górniczych*; Wydawnictwo GIG: Katowice, Poland, 2003.
51. Malinowska, A.; Hejmanowski, R. The impact of deep underground coal mining on earth fissure occurrence. *Acta Geodyn. Geomater.* **2016**, *13*, 184. [[CrossRef](#)]
52. Ścigała, R. *The Influence of Deposit Tectonics on the Distribution on Mining AREA Deformations*; Publ. House of Silesian Univ. of Technology: Gliwice, Poland, 2013.
53. Białek, J. *Algorytmy i Programy Komputerowe do Prognozowania Deformacji Terenu Górniczego*; Wydawnictwo Politechniki Śląskiej: Gliwice, Poland, 2003; p. 199.
54. Strzałkowski, P.; Szafuła, K. Przykład analizy sumowania deformacji terenu górniczego w długim przedziale czasu. *Bezp. Pr. Ochr. Gór.* **2016**, *10*, 14–19.
55. PN-EN 1997-2 Eurokod 7. Projektowanie Geotechniczne. Część 2. Rozpoznanie i Badanie Podłoża Gruntowego. Available online: http://ompkg.pl/wp-content/uploads/2015/02/A_PN-EN-1997-2.pdf (accessed on 20 November 2021).
56. Mermerdaş, K.; İpek, S.; Sor, N.H.; Mulapeer, E.S.; Ekmen, S. The Impact of Artificial Lightweight Aggregate on the Engineering Features of Geopolymer Mortar. *Turk. J. Nat. Sci.* **2020**, *9*, 79–90.